Macromolecules

pubs.acs.org/Macromolecules Article

Synergy in Melting of Initially Disentangled Polymers: Linear versus Ring

Zhiyuan Cheng, Li Peng, Bo Yang, Hong Liu,* Jiajia Zhou,* Xianbo Huang,* and Guojie Zhang*

Cite This: *Macromolecules* 2025, 58, 10164−10180 Read Online

ACCESS | Metrics & More | Article Recommendations

ABSTRACT: Extensive molecular dynamics simulations of the Kremer−Grest model have been conducted to explore kinetic features and molecular mechanisms of the melting process of the initially disentangled linear and ring polymers with varying chain lengths (up to 800) in bulk, with an emphasis on illuminating the specific role of chain topology therein. In the meantime, some interesting issues concerning chain explosions have also been addressed in this study. It is revealed from our computational study that the melting of initially disentangled polymers, both linear ones and rings, is a three-stage process, where there is a synergy of such nonequilibrium processes as globule−coil transitions of polymer chains, polymer interpenetration, and thus formation of nontrivial topological states (i.e., entanglements or threadings) of polymers. We found that the melting of initially disentangled linear polymers seems to be accomplished through chain explosions, while such a picture is obscure for the ring case. In the linear case, it is through sufficient "releasing" of the two chain ends that the disentangled linear chains become able to explode for arriving at their well-equilibrated coil conformations, while chain expansion of ring polymers during the melting occurs with the aid of the formation of more wrinkled conformations due to the absence of chain ends. Moreover, it is concluded that a concomitant development of polymer interpenetrations essentially acts as a requisite for the occurrence of chain expansion during the melting, and a cooperation of chain expansion and interpenetrations leads to the emergence of entanglements in the linear systems and threadings in the rings.

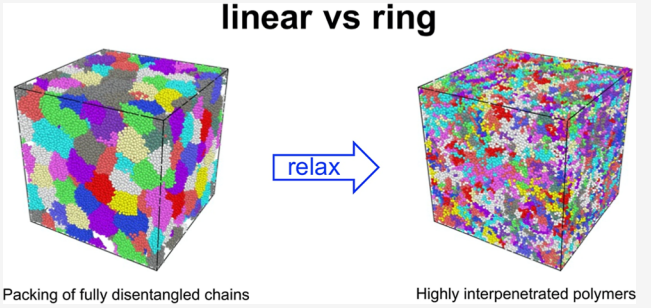

1. INTRODUCTION

A strong interpenetration of polymer chains,[1−6] an emergent phenomenon in dense systems (e.g., semidilute and concentrated polymer solutions, polymer melts, etc.) stemming from a combinational effect of large spatial extent of polymers and space-filling requirement, is the most distinct packing feature of polymer materials compared to other classes of materials, either soft or hard. It is essentially the chain interdigitation that ultimately gives rise to many valuable facets of conformational, structural, thermodynamic, rheological, and other physical properties of many-chain polymer systems.[6] In particular, interpenetration of polymer chains underlies many nontrivial behaviors of, among others, the statics and dynamics of densely packed polymer systems. For instance, the chain interpenetrations, along with the uncrossability of the chains, give rise to an emergence of polymer entanglements in linear flexible polymer systems.[1−4,6] As a consequence, the motion of a linear polymer in melts or concentrated solutions is a one-dimensional random walk (reptation) within a tube.[1,2] The degree of chain interpenetration can be characterized by the invariant degree of polymerization,[7] $\bar{N}$, the root of which approximately quantifies the number of chains interdigitated with a tagged chain within its pervaded volume. More interestingly, the number of entanglements per chain is found to be proportional to the degree of polymerization of the chains. Chain interpenetration also results in unique features of densely packed ring polymers.[5,8] For example, dense packing and the topological constraints of ring polymers in melts lead to fractal crumpled conformations of the rings, where dependence of the radius of gyration of rings on the chain length N follows a scaling law, i.e., $R_g \sim N^{\nu}$, with, however, ν being N-dependent and ranging from approximately 2/5 (for the short chain length) to 1/3 (for infinitely long chains).[9−11] Furthermore, the ring polymers, especially those long ring chains, exhibit a strongly segregated packing structure in a melt.[9] Nevertheless, interpenetration of ring polymers can still occur to some extent, and the degree of chain interpenetration[7] might be enhanced when the chain length becomes larger. As a consequence of ring−ring interpenetration, the threading of a ring by other rings appears

Received: April 20, 2025
Revised: August 19, 2025
Accepted: August 22, 2025
Published: September 5, 2025

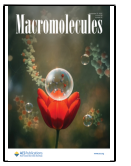

in concentrated solutions or melts of ring polymers, which has been identified in computational studies during the past years.[12,13] It is concluded that quantitatively the number of threadings scales with the chain length of rings and thus becomes considerable for long ring systems.[8]

Development of chain interpenetration from an initially noninterpenetrated (i.e., disentangled) packing of macromolecular chains during the melting is not only an interesting topic in fundamental polymer physics but also plays a key role in ubiquitous processes, such as welding[14] and sintering,[15] of polymeric materials in many practically important applications. Revealing the molecular-level details underlying the kinetics of chain intertwining could contribute to basic knowledge in polymer physics and be helpful for a rational design of high-performance polymeric materials as well. So far, unfortunately, research on this topic is dominantly focused on systems of linear polymers. For a welding process of two interfaces of amorphous linear polymers, experimental studies revealed that the mechanical properties of the welded material strongly depend on the molecular weight of the polymers and the welding time, t_w. Specifically, it is found[16−18] that fracture toughness and shear stress at failure of the welded material scale with the welding time as $t_w^{1/4}$, due to entanglement formation through diffusion of the polymer chains across the interface. Typically, the welding time needed for the final product to recover its corresponding bulk material properties (e.g., fracture toughness) is on the order of the reptation time of the polymer chains.[19] Consequently, the welding of very long-chain interfaces is expected to be a tedious and slow process. Very recently, however, Christakopoulos et al.[16] found that, interestingly, depositing a small amount of disentangled ultrahigh molecular weight polyethylene (UHMWPE) powder at the UHMWPE interface can simply result in an anomalously fast joining of the interface, i.e., buildup of adhesive fracture energy of the welded materials is orders of magnitude faster compared to reptation-driven diffusion of chains at the interface. Similarly, engineering polymers with high molecular weight, e.g., UHMWPE, showing a promising performance, cannot be easily processed by conventional melt processing methods such as injection or extrusion because of their extremely high viscosity due to high entanglement density. Sintering of initially low-entangled or disentangled polymers, inspired by the powder metallurgy of refractory metals, acts as an indispensable way of effectively processing such polymeric materials. It is during the sintering of the low-entangled/disentangled polymers that the chain interpenetration and reentanglement are right developed. For the case of linear polymers, for instance, a controversy still remains on how fast the chain entanglement density is recovered during the sintering process of disentangled/low-entangled polymers. Interrupted shear flow experiments by Roy and Roland[20] and others[21] have been conducted to investigate reentanglement kinetics of linear molten polymers. In experiments by Roy and Roland,[20] the shear flow is halted after steady state is achieved, when polymers have been disentangled to some extent, and the material is held for a period of time, allowing for the occurrence of polymer reentanglements, before resumption of the shearing. The degree of recovery of the stress overshoot in the interrupted shear flow experiments dictates the extent of the recovered entanglement density compared to its initial value, i.e., a full recovery of the polymer entanglements corresponds to a fully reproduced stress overshoot. Authors finally[20,21] concluded that the time for a full polymer reentanglement from the disentangled/low-entangled state is much longer, e.g., more than 1 order of magnitude,[20] than the linear relaxation time (i.e., the reptation time) of the polymer melt at equilibrium. Similar conclusions have also been made in other studies concerning reentanglement processes of disentangled linear polymer solutions[22,23] and melts,[24] freeze-dried linear polymers.[25] These findings that the kinetics of entanglement recovery of disentangled polymers is a very slow process are, however, highly contrasted with another group of experimental and computational studies which revealed a very fast equilibration of the polymer entanglements during relaxation of the disentangled/low-entangled state of linear polymers. Perhaps the first study revealing the fast equilibration of the polymer entanglement dates back to almost 40 years ago, when an almost instantaneous loss of ultra-drawability of low-entangled polymers was reported after melting and recrystallization of solution-cast UHMWPE.[26] This conclusion was further confirmed in an experimental work conducted a few years later.[27] Barham and Sadler.[28] investigated the melting process of single crystals of (i.e., disentangled) polymers, during which polymer chains are expected to undergo intermixing and reentanglement, by measuring the evolution of gyration radius by neutron scattering. They concluded that chains expand very rapidly from folded to random coils, whose time scale is on the order of seconds and is also independent of molecular weight.

To explain the ultrafast melting process of the initially disentangled (and crystallized) polymers observed in experiments, P. G. de Gennes[29] proposed a theoretical model in 1995. In de Gennes' model, each chain invents its own tube during one Rouse time, thus leading to the ratio of the equilibration time to the reptation time being proportional to N/N_e, with N_e denoting the entanglement length. Furthermore, it was theoretically predicted that the time evolution of the radius of gyration of the chains follows a certain scaling law, $R_g \sim t^{\alpha}$ with $\alpha = 1/4$. By that, a chain explosion (or called melting explosion) picture was established, which afterward has been employed by experimentalists to successfully explain their experimental findings in both the sintering[26−28] and some of the welding processes[16] mentioned above. We stress here that, nevertheless, an unambiguous definition of chain explosion was not given by de Gennes himself in the paper,[29] unfortunately. Therefore, we silently assume that the picture of "chain explosion" could be encountered as long as two requirements get fulfilled: (i) the time scale of conformational expansion is shorter than its longest relaxation time in the equilibrated liquid state; and (ii) chain conformations expand in space (measured by radius of gyration) with time during the melting process following a scaling behavior, i.e., $R_g \sim t^{\alpha}$ with $\alpha > 0$. So far, however, the scenario of de Gennes' explosion, especially concerning the second point above-mentioned (i.e., $R_g \sim t^{\alpha}$), upon melting of the disentangled linear polymers has not been completely and unambiguously verified in literature.[30,31]

Considering ring polymers exhibit very distinct features in conformational statics and dynamics,[8−13,32] chain packing structures in a melt at equilibrium,[33] it is thus reasonable to expect that a disentangled ring polymer system could also display some uniqueness in kinetics during its approach to an equilibrium state (i.e., melting). Illuminating the development kinetics of chain interpenetration of disentangled ring polymers would shed light on our understanding of the specific role of chain topology in determining the molecular characteristics of

https://doi.org/10.1021/acs.macromol.5c01047
Macromolecules 2025, 58, 10164−10180

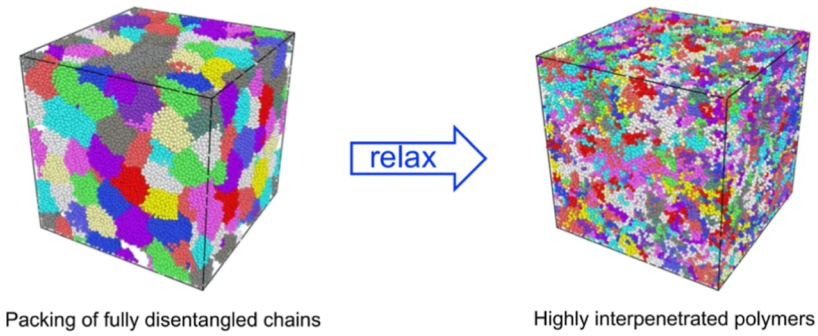

Figure 1. Schematic illustration of the melting process of the densely packed disentangled polymers. After a certain time, the system will ultimately arrive at its equilibrated state characterized by strong interpenetration of the polymer chains. Polymer segments denoted by the same color are those belonging to the same chain as well.

such a nonequilibrium process in general. From another perspective, such obtained knowledge about ring polymers, where there are no chain ends along the chain, could also be useful for a deeper understanding of reentanglement kinetics of disentangled linear polymer melt in general. As far as we have learned, however, the kinetics of chain intermixing of disentangled ring polymers has not been studied yet in the literature.

In this work, we carry out extensive molecular dynamics simulations of the Kremer-Grest model to explore kinetic features, if existing, and illuminate the molecular mechanisms of the melting process of the initially disentangled linear and ring polymers in bulk, aiming to clarify the specific role of chain topology therein. Meanwhile, we try to check whether the chain-explosion scenario, which was initially proposed by de Gennes to explain experimental observations of the sintering of semicrystalline polymers, occurs in our computational systems; and if yes, what are the specific molecular origins and mechanisms underlying its happening. With our computational investigation, we arrive at the following findings: (i) the melting of initially disentangled polymers, either linear ones or rings, is a three-stage process; (ii) there is a synergy of nonequilibrium processes, including conformational changes of polymer chains, polymer interpenetration, and formation of nontrivial topological states (i.e., entanglements or threadings) of polymers during the melting; (iii) the melting of initially disentangled linear polymers seems to be accomplished through chain explosions, while such a picture is obscure for the ring case. This paper is organized as follows. In Section 2, the computational model and simulation details are provided, and results and discussion are given in Section 3. The paper is finally closed with the conclusions in Section 4.

2. MODEL AND COMPUTATIONAL DETAILS

We investigate the melting process (i.e., relaxation) of the disentangled polymers initially densely packed in the system, as illustrated in Figure 1. The polymer chains, either linear or ring, are described by the Kremer−Grest (KG) model,[32] which has been widely used to study the dynamics of polymers with topological constraints, ranging from entangled linear polymers[34−38] and ring polymers[9,39,40] to recently mechanically interlocked polymers.[41−50] Within the Kremer−Grest model, interactions between any two segments in polymers are given by a purely repulsive interaction (Weeks−Chandler−Anderson potential, WCA)

$$U_{\mathrm{WCA}}(r) = \begin{cases} 4\varepsilon[(\sigma/r)^{12} - (\sigma/r)^{6}] + \varepsilon, & r \le r_{\mathrm{c}} \\ 0, & r > r_{\mathrm{c}} \end{cases} \quad (1)$$

and those bonded segments along a chain interact through a finite extensible nonlinear elastic potential (FENE)

$$U_{\mathrm{FENE}}(r) = \begin{cases} -0.5kR_0^2\ln[1 - (r/R_0)^2], & r < R_0 \\ \infty, & r \ge R_0 \end{cases} \quad (2)$$

with $k = 30\ \varepsilon/\sigma^2$, $R_0 = 1.5\sigma$, and $r_{\mathrm{c}} = 2^{1/6}\sigma$. Thus, the time unit of the model is $\tau = \sigma\sqrt{m_{\mathrm{s}}/\varepsilon}$, where k_{B} is the Boltzmann constant and m_{s} is the mass of a segment. In the systems, there are n polymer chains, each with N segments, occupied in a computational box of volume V, such that the number density of polymer segments is $\rho_0 = 0.85\ \sigma^{-3}$. The number of chains, n, ranges from 100 to 200, such that the edges of the simulation boxes are larger than twice the radii of gyration of the polymers under study. Throughout all the simulations, temperature is kept constant as $T = 1.0\ \varepsilon/k_{\mathrm{B}}$, which is fulfilled using a Langevin thermostat with a friction coefficient $1.0\ \tau^{-1}$ within a cubic box with periodic boundary conditions in the three dimensions. The velocity Verlet algorithm is employed to integrate Newton's equations of motion with a time step of 0.01τ.

Initial configurations of the systems, i.e., the densely packed, disentangled polymers in systems, are set up by following two steps. First, a fully collapsed, globular conformation of the polymer (either linear or ring) is generated via simulation of a single chain in an implicitly poor solvent, i.e., through switching the WCA interactions to the Lennard-Jones potentials, by which the nonbonded interactions between polymer segments are of an attractive nature on short length scales. Then, the generated globular configuration of the single chain is copied and randomly packed together in a dilute solution, which thereafter undergoes a gradual compression within $10^5\ \tau$ until the required concentration, i.e., $\rho_0 = 0.85\sigma^{-3}$, is realized. During such operation, we note that the intrachain interactions are always kept attractive, while segments from different chains interact via WCA. After the initial configuration of the disentangled polymers in a melt is prepared, all the Lennard-Jones potentials used are switched to the WCA potentials when the melting process just starts, with $t = 0$. At least eight parallel simulations have been carried out for a given system in order to obtain data with proper statistics.

Characterization of topological states of polymers is conducted in the following. For the linear case, information

https://doi.org/10.1021/acs.macromol.5c01047
Macromolecules 2025, 58, 10164−10180

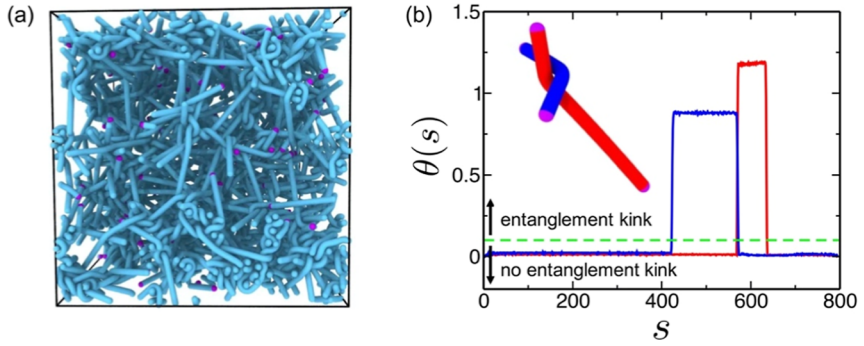

Figure 2. (a) Representative final configuration from a primitive path analysis (PPA) of an equilibrated linear polymer system with $N = 800$. (b) Variation of values of local angle $\theta(s)$ with respect to s ($s \in [1, N-4]$) for two entangled chains, whose PPA conformations are given in the inset. Appearance of one entanglement kink corresponds to a continued region with a positive value of $\theta(s)$, i.e., $\theta(s)>0.1°$.

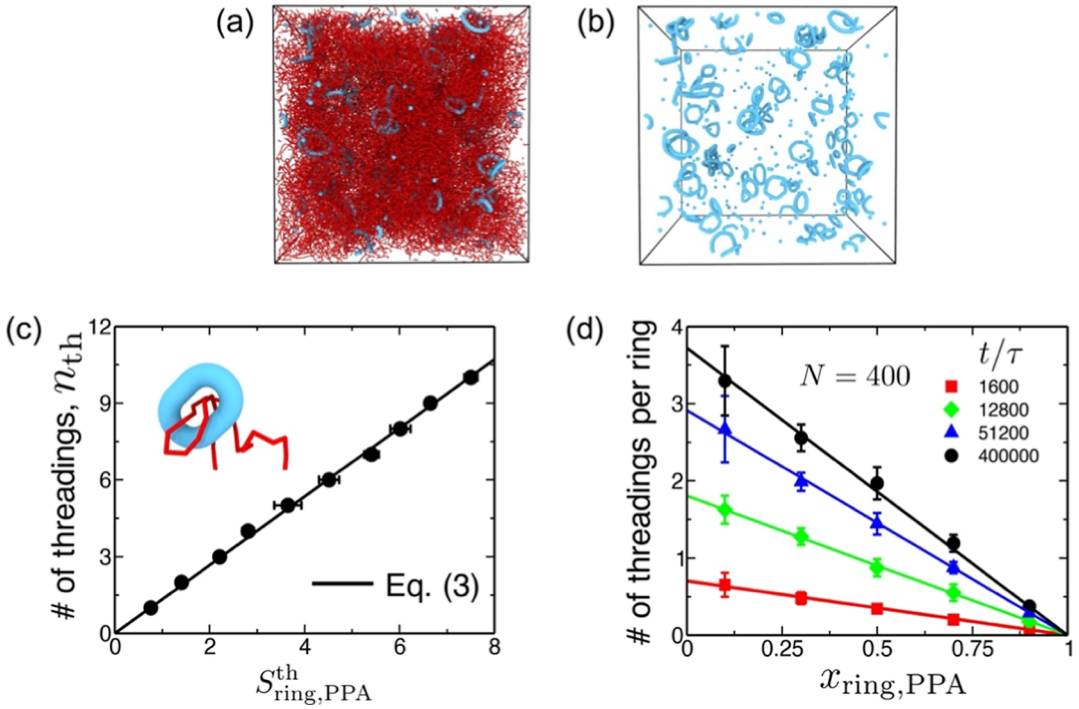

Figure 3. (a) Final configuration from a primitive path analysis (PPA) of a ring polymer system with $N = 800$, after half of the rings (denoted in blue color), i.e., $x_{ring,PPA} = 0.50$, going through a PPA operation. The rest of the chains are shown in red. (b) Chain conformations of half of the rings after PPA. (c) Relationship between the number of threadings per chain and $S^{th}_{ring,PPA}$, a quantity proportional to the effective cavity area of PPA conformation of the threaded ring. (d) Number of threadings per chain calculated by eq 3 as a function of $x_{ring,PPA}$ during the melting process of a system composed of initially disentangled rings with $N = 400$.

on polymer entanglements in systems is obtained through carrying out the standard primitive path analysis (PPA),[51,52] in which molecular dynamics simulations are carried out at a very low temperature, e.g., $T = 0.001\ \varepsilon/k_B$, when the intrachain excluded-volume interactions are disabled but the interchain excluded-volume interactions keep unmodified under a condition of fixing chain ends in space. Figure 2a shows a typical snapshot of chain conformations after PPA implementation mentioned above. Then, the conformational feature of each PPA chain is quantified by measuring local angles, $\theta(s)$ with $s \in [1, N-4]$, formed by two vectors, $\mathbf{r}_{s,s+2} \equiv \mathbf{R}_{s+2} - \mathbf{R}_s$ and $\mathbf{r}_{s+2,s+4} \equiv \mathbf{R}_{s+4} - \mathbf{R}_{s+2}$, where $\mathbf{R}_i$ denotes the spatial coordinate of the i-th segment along the chain backbone. Figure 2b provides a typical variational behavior of $\theta(s)$ with respect to s for the two selected entangled chains. It is clearly seen that value of $\theta(s)$ remains effectively zero for those location not close to the entanglement kink point, where near to and within the entanglement kink region the corresponding $\theta(s)$ continuously stays positive for a certain range of s. Here, one entanglement along a chain can be identified as long as continued positive values of $\theta(s)$, i.e., $\theta(s)>0.1°$, are found. With such a methodological concept, one can easily learn that there is one entanglement for each chain shown in the inset of Figure 2b, and the entanglement positioning along the two chains can also be extracted from the curves of $\theta(s)$ as a function of s.

To identify the topological state (i.e., ring−ring threading) of ring polymers, a further modified PPA methodology is implemented. Because of the absence of chain ends in ring polymers, the conventional PPA operation can be carried out merely without fixing chain ends. Furthermore, only a proportion, $x_{ring,PPA} \in (0,1)$, of the ring polymers is selected to go through the PPA operation, because otherwise all the ring

https://doi.org/10.1021/acs.macromol.5c01047
Macromolecules 2025, 58, 10164−10180

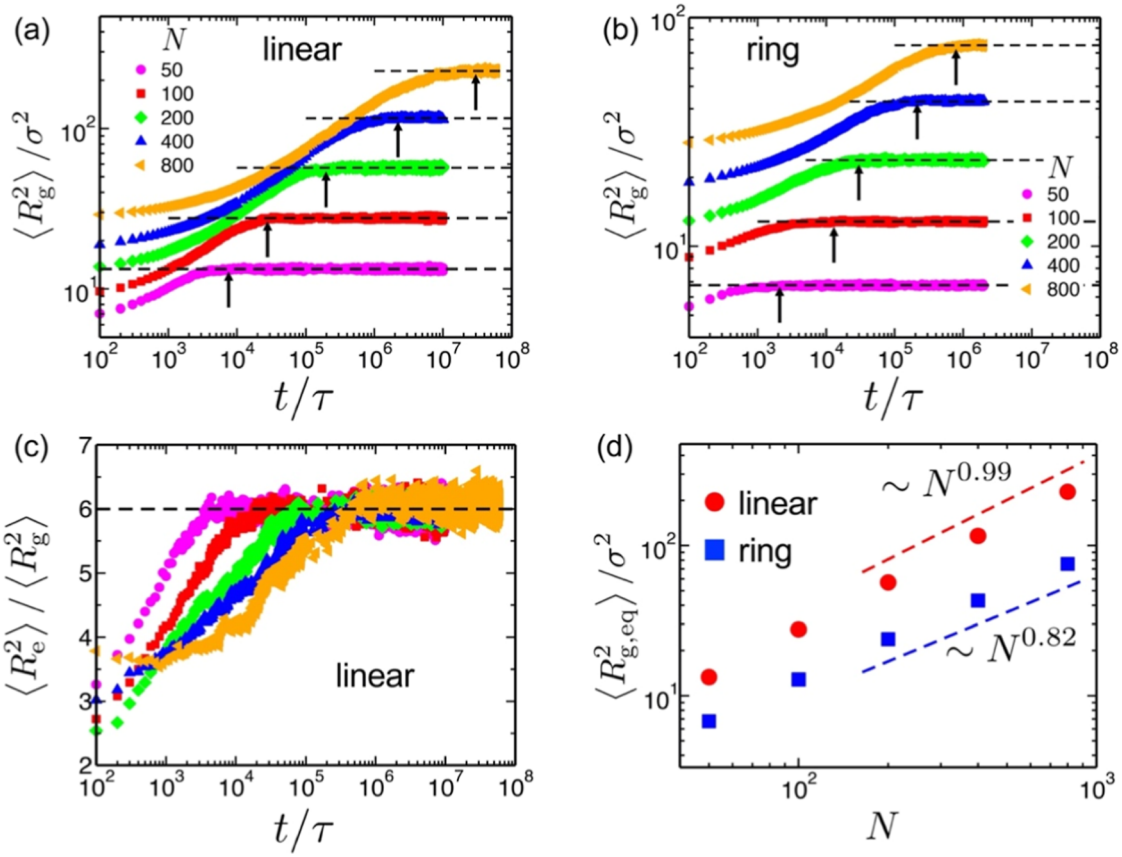

Figure 4. Time evolution of the mean-square radii of gyration, $\langle R_g^2 \rangle$, of the initially disentangled polymers, linear (a) and ring (b), with chain lengths N = 50, 100, 200, 400, and 800. Variation of $\langle R_e^2 \rangle / \langle R_g^2 \rangle$ as a function of the melting time for the linear case is given in (c), where $\langle R_e^2 \rangle$ denotes the mean-square end-to-end distance of the linear polymers. (d) Equilibrated mean-square radii of gyration, $\langle R_{g,eq}^2 \rangle$, as a function of chain length, N.

conformations would be evolved into single points during PPA, from which no information about the topological states of ring polymers would be extracted. Figure 3a provides one typical configuration of a ring polymer system with chain length N = 800 after such modified PPA operation is carried out by setting $x_{ring,PPA}$ = 0.5, where conformations in red/blue colors are those rings without/with undergoing PPA operations. A clearer illustration of the configuration is shown in Figure 3b, in which only those rings that underwent PPA operation are shown. Intuitively, we assume the number of threading chains for a threaded ring, n_{th}, is given by

$$n_{th} = aS^{th}_{ring,PPA} \tag{3}$$

Here, $S^{th}_{ring,PPA}$ can be calculated from the coordinates of polymer segments after PPA operation by $S^{th}_{ring,PPA} = \frac{1}{N}\sum_i (|\mathbf{R}_i - \mathbf{R}_{cm}| - 0.485)^2$, in which $\mathbf{R}_i$ and $\mathbf{R}_{cm}$ denote spatial coordinates of the i-th segment and center of mass of the tagged ring, respectively. Here, 0.485σ would be taken as the radius of polymer segments, which is calculated as half of the bond length (i.e., 0.97σ) of the polymer chain within the Kremer−Grest model. By definition, therefore, $S^{th}_{ring,PPA}$ could be roughly seen as a quantity proportional to the cavity area of the PPA conformation of the threaded ring. Figure 3c represents values of the cavity area of the PPA conformation of a given ring threaded by n_{th} other rings. It is concluded from Figure 3c that the above assumption, i.e., eq 3, is indeed verified, and the parameter $a \approx 1.338$ is obtained through fitting data into eq 3. Since we have to choose only a part, i.e., $x_{ring,PPA}$, of all the ring polymers in a system to conduct PPA operation, the true value of the number of threadings per ring, n^0_{th}, should be redistilled with great caution, because the number of threadings should be a value independent of $x_{ring,PPA}$. To proceed with our analysis, it is beneficial to notice that a PPA operation with larger $x_{ring,PPA}$ would result in a more decreased value of n_{th}. This is because, in a case with choosing a larger value of $x_{ring,PPA}$, the probability of finding simultaneously both one threading and its threaded ring under PPA operations is more and more increased. As a consequence of PPA operation, the ring−ring threading, which exists in reality, would more likely disappear after PPA. In a limiting case with $x_{ring,PPA}$=1, therefore, n_{th} would become zero. Theoretically, it is expected that the true value of the number of threadings per ring, n^0_{th}, should be recovered through extrapolation when $x_{ring,PPA}$ goes to zero, i.e., $x_{ring,PPA} \to 0$. In order to obtain information about n^0_{th}, we conducted a series of PPA operations with varying $x_{ring,PPA}$ and calculated the number of threadings per ring for a system with N = 400 during the melting process. The corresponding results are given in Figure 3d, where values of n_{th} are shown as a function of $x_{ring,PPA}$, i.e., $n_{th} = n_{th}(x_{ring,PPA})$. It is easily seen that indeed n_{th} value decreases with increasing $x_{ring,PPA}$, and interestingly, there is a linear relationship between values of n_{th} and $x_{ring,PPA}$, which successfully confirms the expectation above-mentioned, i.e., $n_{th} \to 0$ when $x_{ring,PPA} \to 1$. Therefore, one can readily derive the true value of n^0_{th} through

https://doi.org/10.1021/acs.macromol.5c01047
Macromolecules 2025, 58, 10164−10180

$$n_{th}^{0} \approx \frac{n_{th}(x_{\mathrm{ring,PPA}})}{1 - x_{\mathrm{ring,PPA}}} \tag{4}$$

Throughout all our PPA operations, we choose $x_{\mathrm{ring,PPA}} = 0.50$, and thus, $n_{th}^{0} = 2n_{th}(0.5)$.

3. RESULTS AND DISCUSSION

The melting of initially disentangled polymers is accomplished through a variety of nonequilibrium processes. These processes include conformational changes of polymer chains (i.e., globule−coil transition), interpenetration (i.e., intermixing) of polymers, and thereafter emergence of nontrivial topological states of polymers (i.e., entanglements in the case of linear chains, and chain threadings for ring polymers). Here, we endeavor to deliver a comprehensive picture of the synergy of the above-mentioned nonequilibrium processes and thus achieve an understanding of the concerted polymer dynamics. Importantly, we also aim to elucidate the specific effect of chain topology, linear versus ring, in determining the kinetic features of the melting of initially disentangled polymers. Meanwhile, we try to examine whether the chain explosion initially proposed by de Gennes[29] is also involved in our systems, and if yes, to clarify the underlying detailed molecular pictures of it.

3.1. Conformational Changes of Polymers during the Melting. It is naturally expected that the initially disentangled polymers with globular conformations, either linear or ring, would undergo conformational changes for relaxation during the melting process. Figure 4a,b provides variation of mean-square radii of gyration, $\langle R_g^2 \rangle$, of linear and ring polymer chains (with chain length N ranging from 50 to 800) in melts as a function of the melting time, t, respectively. It is clearly seen in Figure 4 that the two cases of disentangled polymers, although with distinct chain topologies, share common characteristics in terms of kinetics: (i) $\langle R_g^2 \rangle$ of the chains all start to increase as soon as the beginning of the melting, i.e., undergoing globule−coil transitions; (ii) the conformational transitions are complete after time τ_{gc}, when the polymer chains reach states with converged values of $\langle R_g^2 \rangle$. In Figure 4c, $\langle R_e^2 \rangle / \langle R_g^2 \rangle$ values for linear polymers finally arrive at $\langle R_e^2 \rangle / \langle R_g^2 \rangle \approx 6$, further indicating an equilibration of the systems. The equilibrated values of mean-square radii of gyration, $\langle R_{g,eq}^2 \rangle$, as a function of chain length, N, are given in Figure 4d for both linear (red circles) and ring (blue squares) cases. It is clearly seen that a scaling law, $\langle R_{g,eq}^2 \rangle \sim N^{2\alpha}$, holds for both cases but with varying α values, i.e., $\alpha \approx 0.50$ and $\alpha \approx 0.41$ for the linear and ring polymers, respectively. These findings are in good agreement with conclusions reported in the literature.[1−5,8,10]

The results given in Figure 4a,b unambiguously show that those disentangled ring polymers take a shorter time to go through the whole relaxation compared to their linear counterparts. Such a conclusion can be seen more easily from detailed information about τ_{gc} given in Figure 5 (solid symbols). Interestingly, scaling laws also seem to exist (denoted by dashed lines in Figure 5) for describing relationships between the equilibration time τ_{gc} and the chain length N. In the case of disentangled linear polymer melts, two different scaling laws,[53] i.e., $\tau_{gc} \sim N^{\alpha}$ with $\alpha \approx 2.0$ for $N \leq 200$ and $\alpha \approx 3.4$ for $200 < N \leq 800$, seem to well describe the variation behavior of τ_{gc} with respect to N at least for systems under study. With such a finding, one might suspect that in the linear case, the polymer chains could reach

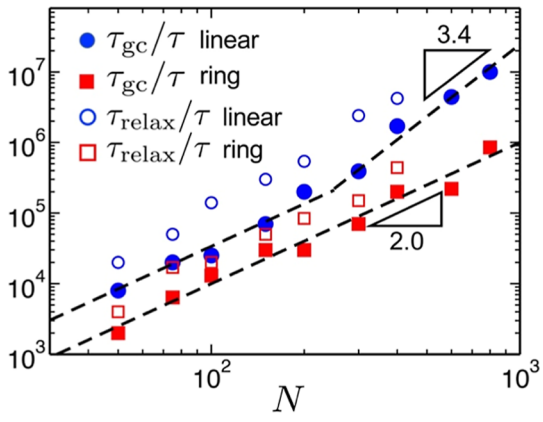

Figure 5. Time needed by the initially disentangled polymers, either linear (solid blue circles) or ring (solid red squares), τ_{gc}, to complete the globule−coil transitions for reaching their corresponding equilibrium states during the melting as a function of chain length, N. Values of the longest relaxation time of well-equilibrated linear (open blue circles) and ring (open red squares) polymers in melts, τ_{relax}, are also added for comparison.

equilibrium in melts through Rouse dynamics and reptation motion for unentangled and entangled polymers,[1−4] respectively. This is, however, in contrast to the scenario of chain explosion proposed by de Gennes,[29] in which a disentangled (and crystallized) polymer approaches its equilibrium conformation through Rouse dynamics in a chain-length-independent fashion. One feasible explanation for such a discrepancy between simulation results and theoretical prediction could be attributed to the difference in initial states of polymers. Namely, it is a single-crystallized polymer as the initial state for a process of reentanglement in de Gennes' theoretical model,[29] while the initial conformations are disentangled globules in our study. Intuitively, conformational expansion of chains in our simulations might not be as easy as that in de Gennes' scenario, e.g., due to likely existing self-entanglement within the chain globule, especially in those long-chain systems.[54] We stress that, nevertheless, this does not necessarily mean that, to arrive at their equilibrated conformations in terms of $\langle R_g^2 \rangle$, the initially disentangled linear polymers take the same time as the longest relaxation time of well-equilibrated polymers in melts. To prove this point, the longest relaxation time, τ_{relax}, of the considered linear polymers with selected chain lengths is also given in Figure 5 (open blue circles) for comparison. Here, the values of τ_{relax} for linear chain systems have been recognized as the time when the mean-square displacements (MSD) of the segments with respect to the center-of-mass of the chain, $g_2(t)$, and the MSD of the center-of-mass of the chain, $g_3(t)$, cross each other. It is clear that at least for the linear polymer systems considered in this work $\tau_{gc} \ll \tau_{relax}$. Quantitatively, $\tau_{relax}/\tau_{gc} \approx 3.0$ for linear polymers with $N \leq 200$ and $\tau_{relax}/\tau_{gc} \approx 4.6$ for those of $200 < N \leq 400$. This finding shows that the melting of initially disentangled linear polymers is indeed a fast process, which is then consistent with the theoretical prediction in de Gennes' explosion scenario.[29] For the linear polymer system with $N = 400$, the chain explosion model predicts $\tau_{relax}/\tau_{gc} = N/N_e \approx 4.7$ (because $N_e \approx 85$ for the linear flexible KG model[37]), being in quantitative agreement with our finding ($\tau_{relax}/\tau_{gc} \approx 4.6$) given above. If not coincident, it suggests that the melting process of the initially disentangled polymers could indeed follow a chain

https://doi.org/10.1021/acs.macromol.5c01047
Macromolecules 2025, 58, 10164−10180

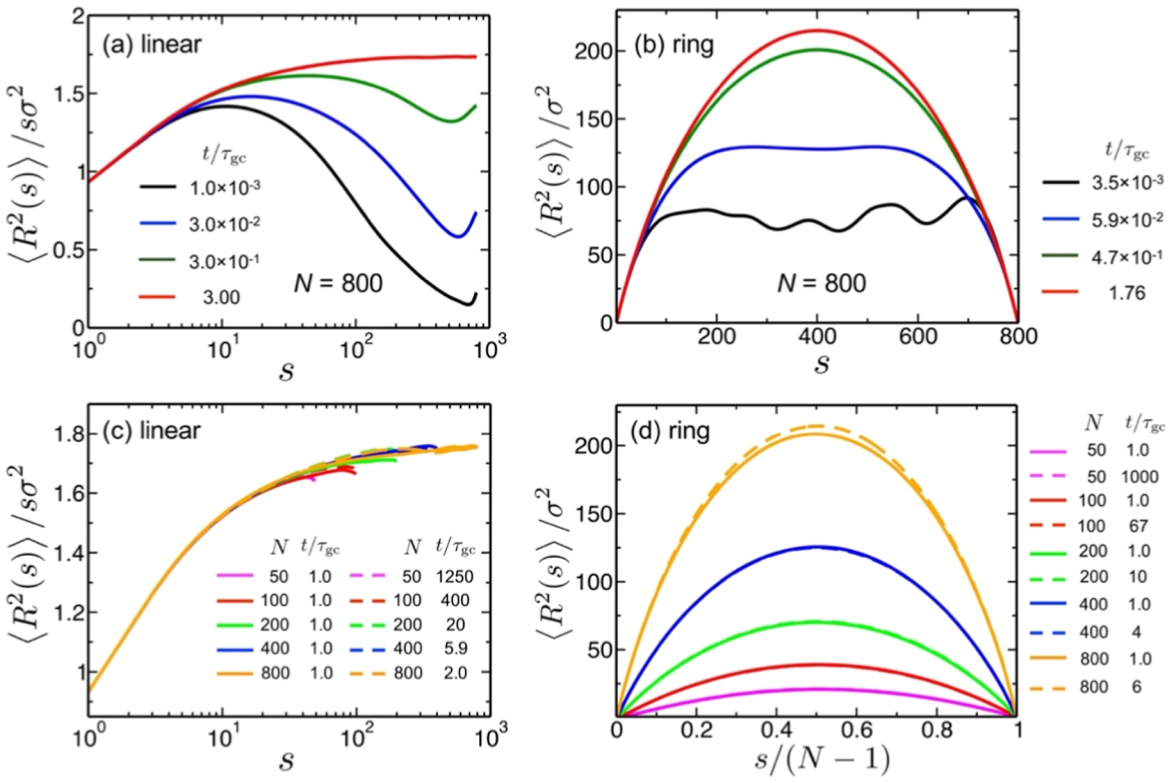

Figure 6. Mean square internal distances, $\langle R^2(s)\rangle$, which measure the mean-square "end-to-end" distances of all polymer strands connected by s consecutive bonds within the same chain, of the linear (a) and ring (b) polymers with $N = 800$, measured long before the systems get equilibrated. The corresponding mean square internal distances measured long after the initially disentangled chains become equilibrated are given in (c,d) for the linear and ring polymers, respectively.

explosion mechanism, even though the chains in our systems are not crystallized ones as in de Gennes' model.[29]

For the case of ring polymers, one can simply notice in Figure 5 that the time required for completion of the globule−coil transitions of initially disentangled ring polymers seems to follow a uniform power law, i.e., $\tau_{gc} \sim N^{\alpha}$ with $\alpha \approx 2.0$ for chains up to $N = 800$. Notably, it has been predicted theoretically[55] that the longest relaxation time, τ_{relax}, of ring polymers in melts exhibits the same scaling law, i.e., $\tau_{relax} \sim t^{2.0}$. Similar to the melting of disentangled linear polymers, results given in Figure 5 show that τ_{gc} is also noticeably smaller than the longest relaxation time of rings in equilibrated melts, τ_{relax}, i.e., quantitatively $\tau_{relax}/\tau_{gc} \approx 2.0$. Here, τ_{relax} was determined as the time when the mean-square displacements (MSD) of the segments with respect to the center-of-mass of the chain, $g_2(t)$, start to converge. The observation of $\tau_{gc} \sim N^{2.0}$ for the ring case may be indicative of some remarkably interesting findings about chain dynamics of ring polymers in melts at equilibrium obtained from molecular dynamics simulations.[39] The authors revealed that the internal structural rearrangement of the ring polymers in melts is a fast process; that is, its corresponding relaxation time, τ^{cc}_{relax}, is much smaller than that needed for them to diffuse their own size. More interestingly, it is concluded in their simulation that there is a power law behavior between τ^{cc}_{relax} and the chain length, N, which is approximately given by $\tau^{cc}_{relax} \sim N^{2.0}$. If not coincident, a combination of our findings and the above-mentioned facts may suggest that the initially disentangled ring polymers can be equilibrated during the melting merely through the internal structural rearrangement of each chain. Apparently, this would be a profound consequence of the circular topology of the ring polymers if that were the case.

Before we move to uncover the detailed features of the melting process and clarify the underlying molecular mechanisms, there is one interesting question worth addressing. Namely, is the onset of convergence of the $\langle R_g^2\rangle$ values, a quantity which merely measures one of the globally conformational properties of polymers, a sign of a full equilibration of polymer conformations at multiple length scales? To answer this question, we resort to a comprehensive inspection of multiscale polymer conformations with the aid of computing their mean-square internal distance, $\langle R^2(s)\rangle$ with $s \in [1, N-1]$, which essentially measures the mean-square "end-to-end" distances of all polymer strands connected by s consecutive bonds within the same chain. Therefore, $\langle R^2(s)\rangle$ stands as a valuable quantity that is capable of faithfully depicting multiscale characteristics of conformations of the polymers. As a consequence, the shape of the mean-square internal distance plot (usually in terms of $\langle R^2(s)\rangle/s$ versus s) becomes so sensitive to distortion/deformation of polymer conformations at any length scale that even a slight deviation of conformations from the corresponding equilibrated one would lead to a noticeable signal in the plot. This is why the mean-square internal distance has been widely employed to evaluate equilibration quality of entangled linear polymer melts in computer simulations[35−38] since Auhl and co-workers[56] first proposed it. The mean-square internal distance plots, $\langle R^2(s)\rangle/s$ with respect to s for linear, and $\langle R^2(s)\rangle$ with respect to $s/N - 1$ for ring polymers with $N = 800$, measured (in terms of t/τ_{gc}) long before when their radii of gyration become saturated, are shown in Figure 6a,b, respectively. One can easily notice a

https://doi.org/10.1021/acs.macromol.5c01047
Macromolecules 2025, 58, 10164−10180

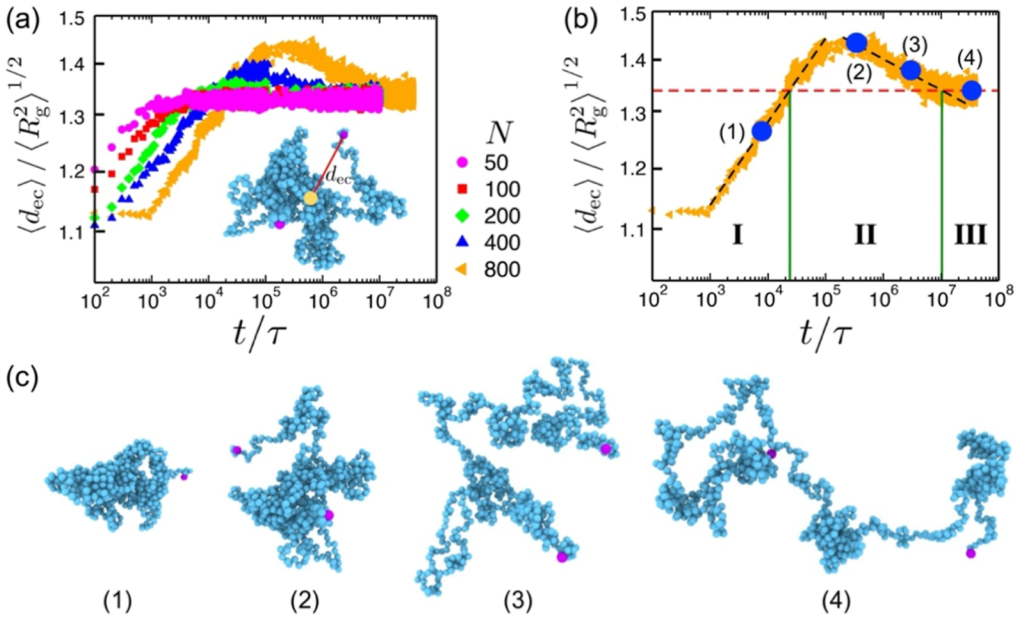

Figure 7. (a) Time evolution of the rescaled distance between chain ends and center of mass, $\langle d_{ec}\rangle/\langle R_g^2\rangle^{1/2}$, for the linear polymers with varying chain lengths N, during the melting process; (b) plot of values of $\langle d_{ec}\rangle/\langle R_g^2\rangle^{1/2}$ versus t for the system with N = 800, as well as the characteristic three stages (I, II, and III); (c) typical snapshots for the system with N = 800 selected in each stage from (b).

remarkable evolution of the mean-square internal distances as a function of the melting time for both the linear and ring polymers. Figure 6c,d provides the mean-square internal distances soon after their radii of gyration become saturated as solid lines for the linear and ring cases, respectively. For comparison, the corresponding results obtained over a time period with $t/\tau_{gc} \gg 1$ (except those systems with N = 800) are also added in Figure 6c,d as dashed lines. It can be seen that, for either linear or ring systems, the mean-square internal distance plots measured soon after and long after when the systems get "equilibrated" (in terms of $\langle R_g^2\rangle$) are sitting on top of each other. This finding essentially means that multiscale conformations of polymer chains in both linear and ring systems can get well-equilibrated during the melting as soon as their globule−coil transitions are finished. Such a fact implies that the radius of gyration can indeed serve as an appropriate quantity for monitoring equilibration quality of the melting process.

Now, we are faced with the central and important question, namely, what are the detailed molecular pictures underlying the melting process (i.e., the globule−coil transitions) of those disentangled polymers? Because of the presence of chain ends in the linear systems, we simply postulate that the globule−coil transitions of the initially globular linear polymers proceed mainly through continuously extending outward of the two chain ends. If such a presumed picture was true, a gradual increase of distance between each chain end and the center of mass of the same chain, d_{ec}, would be seen during the melting process. To test it, we thus monitored the time evolution of the averaged distance, $\langle d_{ec}\rangle$, in the course of melting of the disentangled linear polymers. Figure 7a provides those results by the dimensionless averaged distance, $\langle d_{ec}\rangle/\langle R_g^2\rangle^{1/2}$, with $\langle R_g^2\rangle^{1/2}$ denoting the corresponding radii of gyration measured at the same instant as $\langle d_{ec}\rangle$. Notably, arising (declining) in the $\langle d_{ec}\rangle/\langle R_g^2\rangle^{1/2}$ value indicates that the extent of increasement of $\langle d_{ec}\rangle$ is greater (smaller) than that of increasement of $\langle R_g^2\rangle^{1/2}$. It is concluded from Figure 7a that indeed, chain ends of those initially globular linear polymers move outward continuously with progression of the melting process of all the considered systems at their early stages. One can easily recognize, however, one important difference in the detailed behavior among the systems with varying chain lengths in the intermediate stage. We find that noticeable peaks appear in those intermediated stages at least for systems $N \geq 200$, while no such peak can be clearly recognized in the system with N = 50. Appearance of these peaks essentially means an "overshoot" of the $\langle d_{ec}\rangle/\langle R_g^2\rangle^{1/2}$ curves. At the final stages, values of $\langle d_{ec}\rangle/\langle R_g^2\rangle^{1/2}$ become converged, indicating an equilibration of the systems. Conceptually, the features of $\langle d_{ec}\rangle/\langle R_g^2\rangle^{1/2}$ versus t being uncovered above allow us to divide the whole process of melting into three stages: stage I, stage II, and stage III. This can be demonstrated in Figure 7b, in which the behavior of $\langle d_{ec}\rangle/\langle R_g^2\rangle^{1/2}$ versus t of one selected system (N = 800) is separately plotted again. As seen in Figure 7b, stage II corresponds to the region of overshoot of the $\langle d_{ec}\rangle/\langle R_g^2\rangle^{1/2}$ values, while the other two stages, i.e., stage I and stage III, are right separated by stage II. Technically, boundaries of these stages are determined as crossing points between the black dashed lines and the red dashed lines shown in Figure 7b. Here, the two black dashed lines are obtained by fitting data to a power-law function, i.e., $\langle d_{ec}\rangle/\langle R_g^2\rangle^{1/2} \sim t^{\alpha}$, for the early and intermediate stages, and the red dashed line accounts for the converged value of $\langle d_{ec}\rangle/\langle R_g^2\rangle^{1/2}$ at much later times. One can notice that stage I occupies most parts of $\langle d_{ec}\rangle/\langle R_g^2\rangle^{1/2}$ arising in Figure 7b. By recalling the physical meaning of $\langle d_{ec}\rangle/\langle R_g^2\rangle^{1/2}$ arising (and declining) as mentioned early, we learn, it is in stage II that the extent of chain dimensional increasement

https://doi.org/10.1021/acs.macromol.5c01047
Macromolecules 2025, 58, 10164−10180

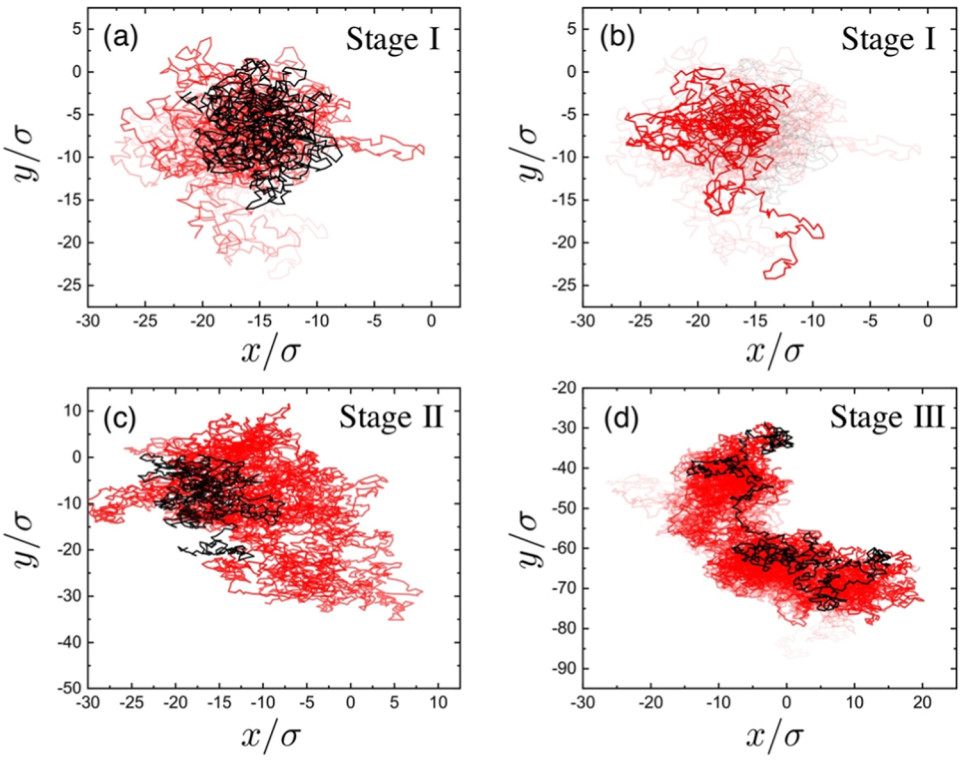

Figure 8. Evolution of chain snapshots of one selected chain in initially disentangled linear polymers during their melting process at stage I (a), stage II (c), and stage (III) (d). Chain snapshots at earlier times are drawn darker in color with the first chain conformation in black. Chain snapshot shown in (b) is one typical conformation at the end of stage I. Polymer conformations shown in (d) are collected during a time period of $2.0 \times 10^5\tau$.

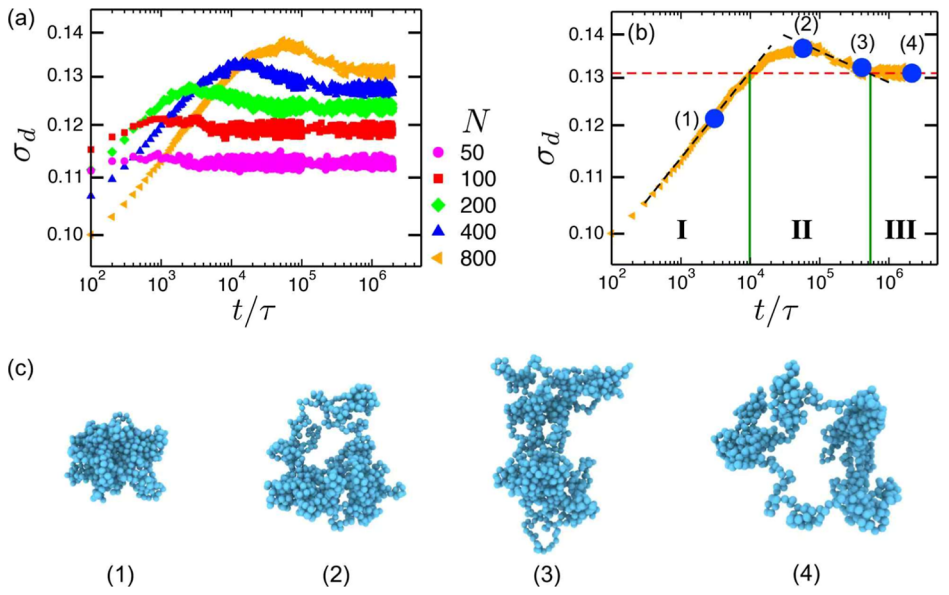

Figure 9. (a) Time evolution of a rescaled (dimensionless) standard deviation of the distance between each segment and the center of mass of the ring, $\sigma_d = [(\langle d_{sc}^2\rangle - \langle d_{sc}\rangle^2)/\langle d_{sc}^2\rangle]^{1/2}$, for the ring polymers with varying chain lengths N, during the melting process; (b) plot of σ_d values versus t for the system with $N = 800$, as well as the characteristic three stages; (c) typical snapshots for the system with $N = 800$ selected in each stage from (b).

starts to overtake that of the distance between chain ends and center of mass of the chain. Four typical snapshots selected from the three stages are also shown in Figure 7c for a pictorial demonstration of the conformation changes of disentangled linear polymers during the melting. Furthermore, Figure 8 provides a direct visualization of what happens for a linear chain ($N = 800$) in the three stages during the melting process. In stage I shown in Figure 8a, chain snapshots at earlier times are drawn darker in color with the initial disentangled one in black. The chain snapshot at later times of stage I is highlighted in Figure 8b, in which one of the chain ends extending outward is easily seen. This picture is very consistent with the arising

https://doi.org/10.1021/acs.macromol.5c01047
Macromolecules 2025, 58, 10164−10180

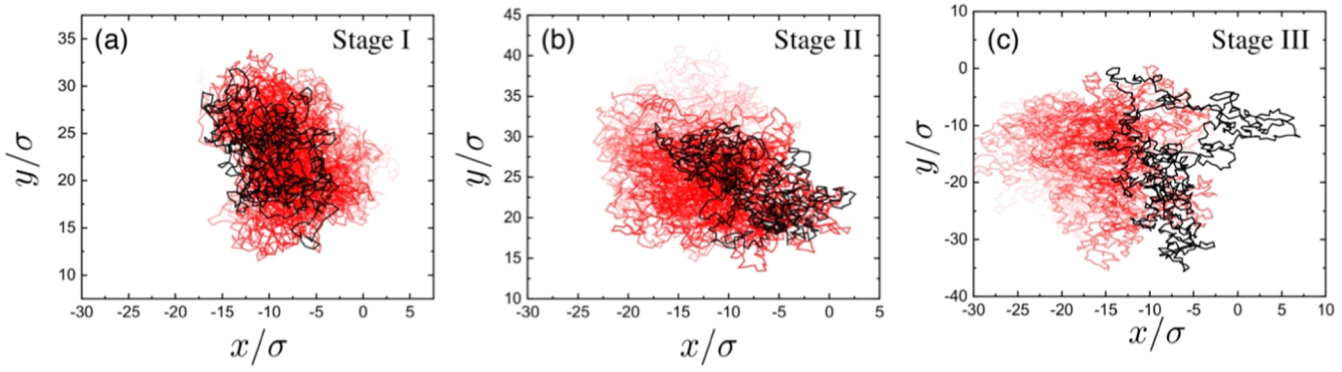

Figure 10. Evolution of chain snapshots of one selected chain in initially disentangled ring polymers during their melting process at stage I (a), stage II (b), and stage (III) (c). Chain snapshots at earlier times are drawn darker in color with the first chain conformation in black. Ring conformations shown in (c) are collected from a time period of $1.0 \times 10^6\tau$.

behavior of $\langle d_{ec}\rangle/\langle R_g^2\rangle^{1/2}$ with respect to t in stage I, as given in Figure 7b. Figure 8c represents a time evolution of chain snapshots in stage II, delivering clear visualizing evidence for a fast chain expansion. With all the molecular pictures revealed, we can conclude that it is through sufficiently "releasing" the two chain ends that the disentangled linear chains become able to expand for arriving at their well-equilibrated conformations.

Similar analysis should be conducted for ring polymers for discovering the corresponding molecular pictures of the initially disentangled rings during the melting. However, the above characterization for the linear case is not directly applicable, due to the absence of chain ends in the ring case. Instead, we resort to looking into the fluctuation of the distance between each segment and the center of mass of the ring, d_{sc}. Specifically, a rescaled (dimensionless) standard deviation of d_{sc}, σ_d, is calculated by

$$\sigma_d = [(\langle d_{sc}^2\rangle - \langle d_{sc}\rangle^2)/\langle d_{sc}^2\rangle]^{1/2} \quad (5)$$

value of which is a characterization of the fluctuation of d_{sc} with respect to its averaged value, $\langle d_{sc}\rangle$. That is, $\sigma_d = 0$ accounts for a perfect circular conformation of the ring polymer, while larger σ_d would correspond to a more wrinkled conformation of the rings. One may readily recognize that $\langle d_{sc}^2\rangle$ is mathematically identical to $\langle R_g^2\rangle$.

Figure 9a gives the variation of σ_d values as a function of the melting time, t, for all of the ring systems under study in this work. It can be seen that, for all the systems considered here, σ_d increases at the early stage of the melting process and reaches peak values, after which it drops gradually to final converged values at the later times. Although this behavior looks similar to its linear counterpart, the physical meaning behind it is qualitatively different. Similar to the linear case, results given in Figure 9a demonstrate that the fluctuation of d_{sc}, σ_d, also undergoes a rise-first-and-then-decline process, and the regions around the peak in Figure 9a correspond to the time periods when ring conformations are the most wrinkled ones. Based on the same criterion employed in Figure 7, three stages can also be defined in the case of ring polymers, as clearly demonstrated in Figure 9b. Very interestingly, it can be learned from Figure 9b that the time region of ring conformations being remarkably wrinkled is right where stage II is located. Indeed, the four representative snapshots (with $N = 800$) provided in Figure 9c verify the wrinkled ring conformation at stage II. Time evolution behaviors of chain snapshots during the three stages are provided in Figure 10, where again chain snapshots at earlier times are drawn darker in color, with the first conformation in each stage in black. All of the above findings lead to the conclusion that the melting of the initially disentangled ring polymers occurs with the aid of the formation of more wrinkled conformations due to the absence of chain ends.

In addition to the three-stage feature, kinetics of the melting process can be further depicted by duration of stage I and stage II, $\tau_{gc}^{\text{stage I}}$ and $\tau_{gc}^{\text{stage II}}$, the values of which can be easily obtained from data given in Figures 7a and 9a according to the definition of the three-stages proposed above. In some sense, stage I can be seen as the preparation stage for stage II, i.e., the former paves the way for the appearance of the latter. Figure 11a provides results about the variation of $\tau_{gc}^{\text{stage I}}$ values with

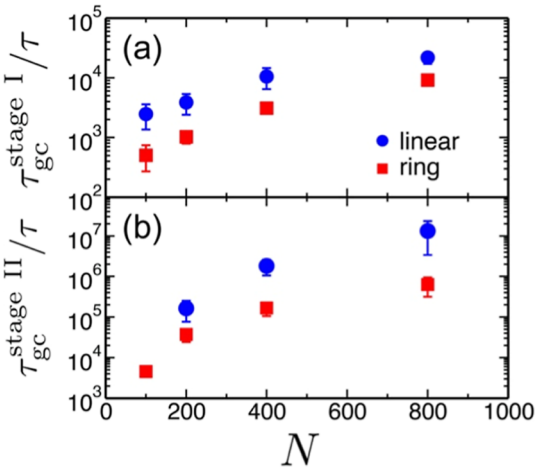

Figure 11. Duration of (a) stage I, $\tau_{gc}^{\text{stage I}}$, and (b) stage II, $\tau_{gc}^{\text{stage II}}$ in the course of evolution of the mean-square radii of gyration, $\langle R_g^2\rangle$, with the melting time, t, of the initially disentangled linear and ring polymers.

respect to chain length N in both cases of linear (solid blue circles) and ring (solid red squares) polymers. It is found that polymers in those systems composed of longer chains also experience a longer duration of stage I, i.e., larger values of $\tau_{gc}^{\text{stage I}}$ for both linear and ring cases. Information on the duration of stage II, $\tau_{gc}^{\text{stage II}}$, can be found in Figure 11b, which leads to a similar conclusion that $\tau_{gc}^{\text{stage II}}$ increases as the chains are longer in all the systems.

https://doi.org/10.1021/acs.macromol.5c01047
Macromolecules 2025, 58, 10164−10180

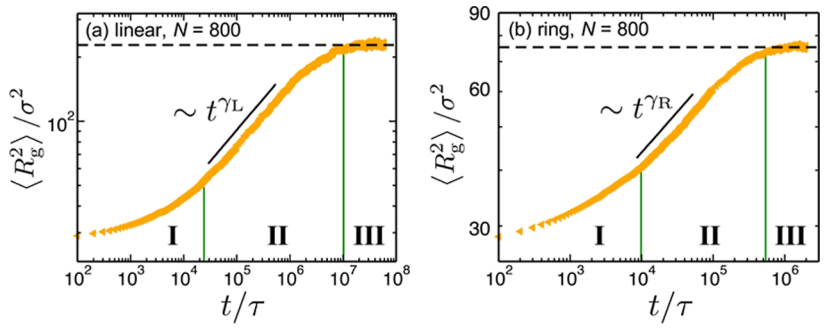

Figure 12. Three-stage feature of the evolution of the mean-square radii of gyration, $\langle R_g^2 \rangle$, with respect to time, t, for both the initially disentangled linear (a) and ring (b) polymers during the melting process. For clarity, only systems with $N = 800$ are selected here for demonstration, without losing generality.

With the three-stage feature of the melting process being uncovered, it is instructive to look back into the time evolution of the radius of gyration for the two cases (linear and ring), investigating the kinetic features of $\langle R_g^2 \rangle$ in each of those distinct stages. Without loss of generality, the evolution of $\langle R_g^2 \rangle$ values of two selected linear and ring polymer systems ($N = 800$) as a function of the melting time, t, is plotted again in Figure 12a,b, respectively. In the meantime, information about the locations of the three stages (stage I, stage II, and stage III) is given in Figure 12 accordingly. As demonstrated in Figure 12, stage I is recognized as the onset of the conformational relaxation of the initially disentangled globular polymers, during which $\langle R_g^2 \rangle$ increases somehow slowly. After that, systems enter stage II, where $\langle R_g^2 \rangle$ values get enlarged in a uniform and fastest fashion. Specifically, there seems to be a scaling law describing the time evolution of $\langle R_g^2 \rangle$ with time in stage II, i.e., $\langle R_g^2 \rangle \sim t^{\gamma}$. Stage III is a time period in which the systems gradually get saturated.

As already shown in Figure 12, conformational dynamics of both linear and ring polymers in stage II display a unique kinetic feature compared to other stages, i.e., $\langle R_g^2 \rangle \sim t^{\gamma}$. Values of scaling exponent γ are provided in Figure 13 for all of the

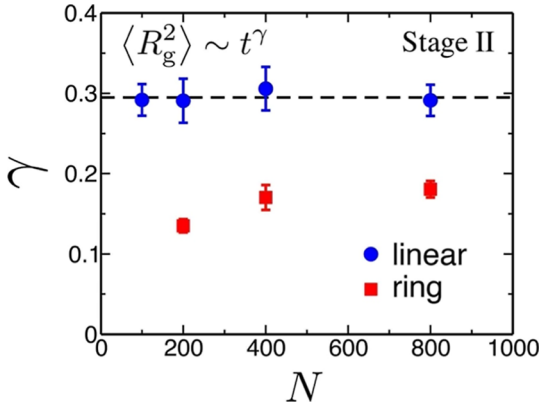

Figure 13. Values of the scaling exponent in $\langle R_g^2 \rangle \sim t^{\gamma}$ for stage II with respect to chain lengths N for both linear and ring cases.

systems under study in this work. One can see that, very interestingly, the scaling exponent γ remains almost constant, $\gamma \approx 0.29$, in the linear case irrespective of the chain lengths, while for ring polymers, as N becomes larger, γ slowly increases but seems to converge toward a constant value $\gamma \approx 0.20$. Furthermore, it is found that the scaling exponent values of the linear chains remains larger than its ring counterparts, i.e., $\gamma_L > \gamma_R$, indicating the disentangled linear polymers expand in a faster fashion compared to the corresponding ring systems. Apparently, such a distinction of the exponent values should be rooted in the difference of chain topology in both cases, and more importantly, it essentially implies that the disentangled linear polymers could undergo a different kind of molecular process from the case of disentangled rings. Such a uniform scaling law, i.e., $\langle R_g^2 \rangle \sim t^{0.29}$, during the melting of the initially disentangled linear polymers is reminiscent of the chain explosion scenario proposed by de Gennes, which predicts that the variation of the mean-square radius of gyration as time follows a scaling law with also a uniform but larger exponent, i.e., $\langle R_g^2 \rangle \sim t^{0.50}$. According to our presumed definition of "chain explosion" in de Gennes' model,[29] combining this finding with the aforementioned results, i.e., a much shorter time is needed for equilibration of the disentangled linear polymers, leads us to conclude: the melting process of the initially disentangled linear polymers proceeds indeed through a chain explosion mechanism, while the chain explosion picture is not that clear in the ring counterpart essentially due to absence of chain ends.

3.2. Development of Polymer Interpenetration and Concomitant Emergence of Nontrivial Topological States. From a polymer physics perspective, the globule−coil transitions of the initially globular polymers are dominantly driven by conformational entropy of the chains since the initially globular states are of very low conformational entropy in nature. Nevertheless, the disentangled polymers, both linear ones and rings, undergo conformational changes during melting in neither isolated states nor dilute solutions. Instead, it is in bulk systems that the globule−coil transitions of the polymer chains proceed for the accomplishment of the melting. That is, initially, all the globular polymers, which could be roughly seen as solid balls, are densely packed together as shown in Figure 1. In this situation, then why/how can the conformational changes of those initially globular polymers happen and, moreover, in such a very efficient manner?

To solve this "puzzle", one insight would be helpful. Thanks to possessing a huge number of conformational degrees of freedom, polymer chains have already been able to rearrange themselves, even though very gradually, as early as the beginning of the melting, when they are densely packed. This stage could correspond to stage I defined in the last section. As the relaxation of the globular polymers proceeds, chain dimensions (e.g., radius of gyration) increase accordingly, resulting in loosing of conformations. As a consequence,

https://doi.org/10.1021/acs.macromol.5c01047
Macromolecules 2025, 58, 10164−10180

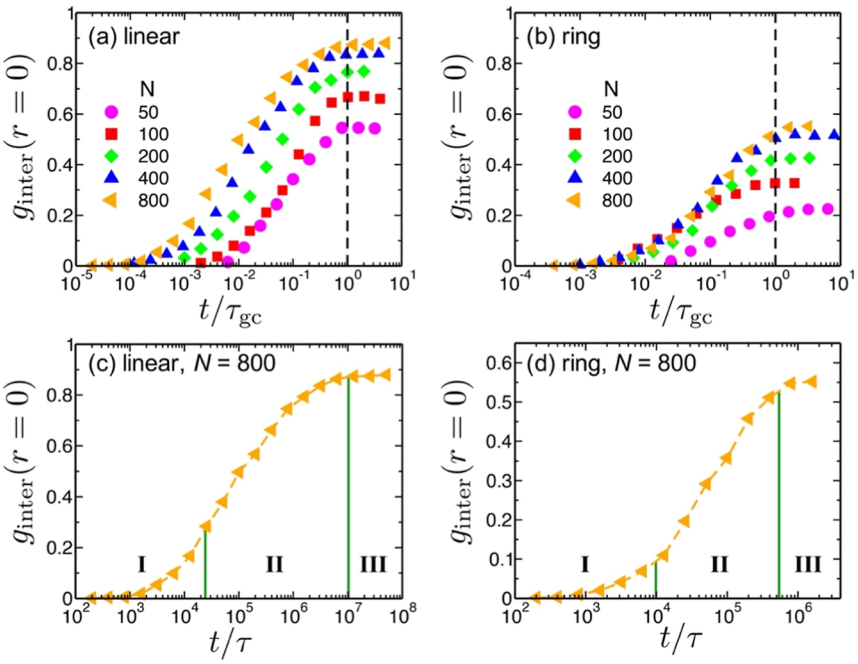

Figure 14. Time evolution of the interchain correlation function at $r = 0$, i.e., $g_{\mathrm{inter}}(r = 0)$, for the linear (a) and ring (b) systems with varying chain lengths; and values of $g_{\mathrm{inter}}(r = 0)$ versus t for the linear (c) and ring (c) systems with $N = 800$.

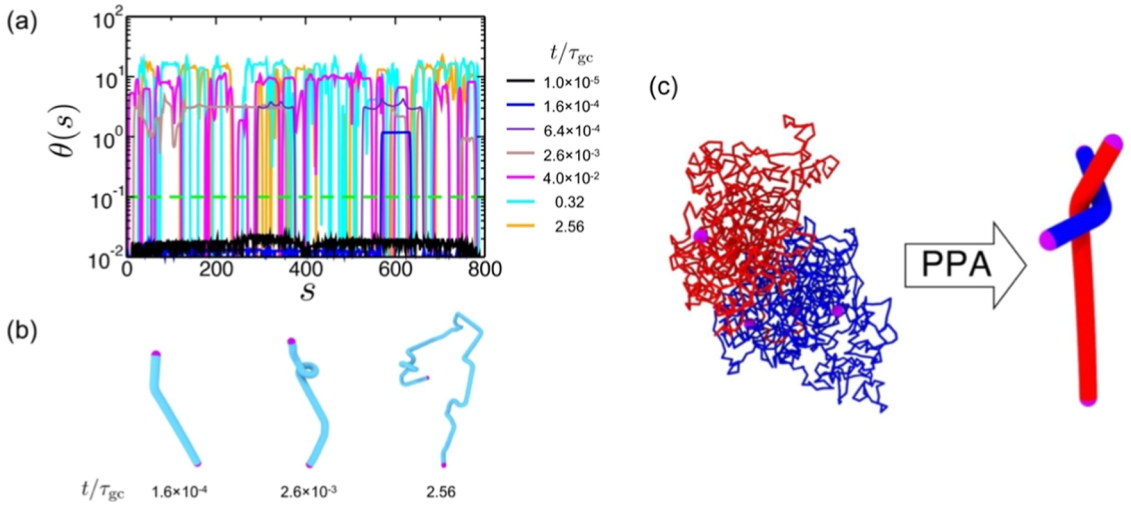

Figure 15. (a) Time evolution of $\theta(s)$ versus s of one representative chain during the melting of initially disentangled linear polymers with $N = 800$. (b) PPA conformations of the chain at different times. (c) Snapshots of the penetrating chain (red) and its neighboring penetrated chain (blue) at $t/\tau_{\mathrm{gc}} = 1.6 \times 10^{-4}$ as well as their configurations after PPA operation.

polymer interpenetrations occur due to the low compressibility of polymer melts. More importantly, the interpenetration of chains can in turn make polymer conformations looser, which subsequently inspires a stronger intermixing of the polymer chains. This would finally lead to an increasingly faster expansion of chain conformations in the course of the melting. We would assign stage II to this happening. In short, once polymer conformational changes (e.g., expansion) are initiated, globule−coil transitions proceed forward with development of chain interpenetrations in a somewhat mutual-cooperative way. To answer the question raised above, therefore, we hypothesize that an early stage (stage I) of polymer conformational changes gives rise to the development of chain interpenetrations, which then essentially stimulates the occurrence of a fast chain expansion at later stages (i.e., stage II) during the melting.

In order to verify/falsify the proposed hypothesis, we need to look into polymer interpenetration and explore the correlation between its kinetics and the appearance of chain expansion. Interpenetration of polymer chains in dense systems can be evidenced by interchain correlations. Here, we defined one interchain correlation function, $g_{\mathrm{inter}}(r)$, which measures the pairwise distribution function between the center of mass of one chain and the coordinates of particles belonging to other chains. Then the degree of polymer interpenetrations would be quantified by the value of $g_{\mathrm{inter}}(r)$ at $r = 0$, i.e., larger $g_{\mathrm{inter}}(r = 0)$, stronger intermixing of polymer chains. Figure 14a,b gives the time evolution behavior of $g_{\mathrm{inter}}(r = 0)$ values for all of the linear and ring systems (with varying chain lengths) under study in this work, respectively. Note here, for a clear comparison of results obtained from systems, that a

https://doi.org/10.1021/acs.macromol.5c01047
Macromolecules 2025, 58, 10164−10180

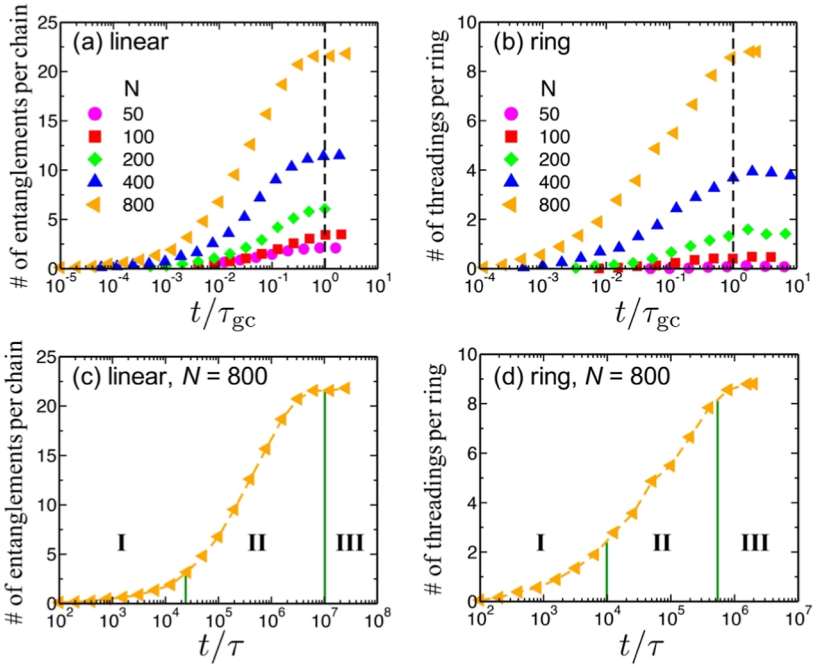

Figure 16. Time evolution of the number of entanglements per chain for the linear (a) and number of threadings per ring (b) of the considered systems with varying chain lengths during the melting; (c,d) corresponding time evolution behavior and the corresponding three characteristic stages for the systems of linear polymers and rings with $N = 800$, respectively.

rescaled, dimensionless time, i.e., t/τ_{gc}, is used here for demonstration as shown in Figure 14a,b. It can be easily seen that for all the systems, both linear ones and rings, g_{inter} $(r = 0)$ increases as the melting progresses and reaches their converged values around $t/\tau_{gc} \approx 1$ as expected, indicating the polymer chains get more and more intermixed in the course of the melting. To explore the correlation between interpenetration and conformational changes (i.e., chain expansion) of polymers, results of g_{inter} $(r = 0)$ as a function of t for the linear and ring systems with chain length $N = 800$ are plotted in Figure 14c,d, where information about the location of the three stages is provided. Interestingly, we found that the time period, i.e., stage II, when polymer conformations change in the fastest way, is right in the region in Figure 14c,d where g_{inter} $(r = 0)$ grows most abruptly after the value g_{inter} $(r = 0)$ is accumulated to some extent in stage I. This finding essentially implies that a fast chain expansion, in either the linear or ring case, cannot happen until polymer chains become interpenetrated to a certain degree. As a conclusion, such a fact verifies the hypothesis proposed above.

As discussed in the Introduction, polymer interpenetration in many-chain systems can essentially result in an emergence of nontrivial topological states,[1−6,8,12,13,32,57−60] i.e., entanglements[57−60] in the linear polymers and threadings[8,12,13,32] in the ring systems. Then, it would be desirable to explore how these topological states appear and evolve kinetically during the melting of the initially disentangled polymers in the bulk. Emergence of polymer entanglements in a disentangled linear chain melt, i.e., a re-entanglement process, could be one of the most interesting topics. For the linear case, to quantify the number of entanglements as well as identify the location of entanglement kinks along a chain backbone, as proposed and carefully tested in Section 2, we resort to measuring local angles, $\theta(s)$ with $s \in [1, N-4]$, of PPA chain conformations. Within this methodology, each entanglement kink can be successfully identified once a (often very rugged) "plateau" of $\theta(s)$ with $\theta(s) > 0.1°$ is found. As a demonstration, Figure 15a provides a time evolution of $\theta(s)$ versus s of one representative chain during a melting of initially disentangled linear polymers with $N = 800$. It can be clearly seen that at time $t/\tau_{gc} = 1.0 \times 10^{-5}$, corresponding to a very early time of stage I, all of values of $\theta(s)$ is below 0.1° (denoted by green dashed line), indicating no entanglement being formed. Very interestingly, it is near the end of stage I, i.e., $t/\tau_{gc} = 1.6 \times 10^{-4}$, that one can easily notice one plateau of $\theta(s)$ appearing (around $s \approx 600$), corresponding to the formation of one entanglement kink along the chain backbone. Figure 15b shows the corresponding PPA conformation of the chain at $t/\tau_{gc} = 1.6 \times 10^{-4}$. Notably, this finding is reminiscent of the above-revealed molecular picture of chain ends extending outward during stage I. To better understand such a consistency, Figure 15c gives chain snapshots of the tagged chain (in red color) as well as its neighboring and later on entangled one (in blue color). On closer inspection, one can notice that indeed at that time $(t/\tau_{gc} = 1.6 \times 10^{-4})$, one chain end of the red chain (or the named penetrating chain) has already entered into, apparently through extending the chain end outward, the spatially occupied region of the blue one (named the penetrated chain). As a consequence, one entanglement between the red and blue chains is formed, as evidenced by their PPA conformations, as given in Figure 15c. With this picture revealed, one can then understand why the location of the entanglement kink just formed is near one end of the red chain. One can also easily understand that the entanglement kink is positioned not necessarily near one of the two chain ends of the blue one. From a probability perspective, it is rather more likely to have the entanglement kink found (far) from the chain ends of the penetrated chain, as demonstrated in Figure 15c. With the melting proceeding, one can learn in Figure 15a that more and more rugged plateaus of $\theta(s)$ appear after $t/\tau_{gc} = 1.6 \times 10^{-4}$, i.e., corresponding to stage II and stage III, suggesting the

https://doi.org/10.1021/acs.macromol.5c01047
Macromolecules 2025, 58, 10164−10180

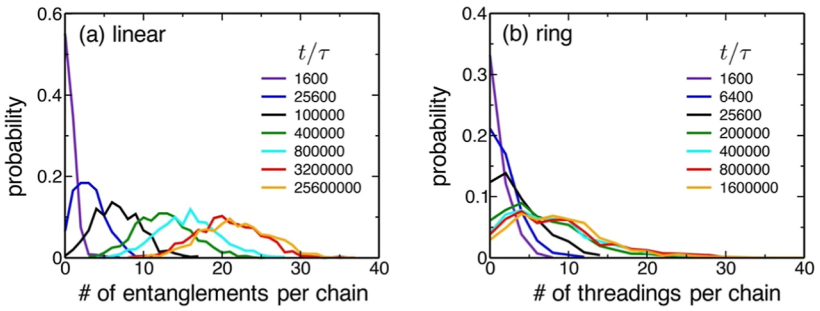

Figure 17. Evolution of probability distribution of number of entanglements (a) and threadings (b) per chain varying with time during the melting process of initially disentangled linear and ring polymers (with N = 800), respectively.

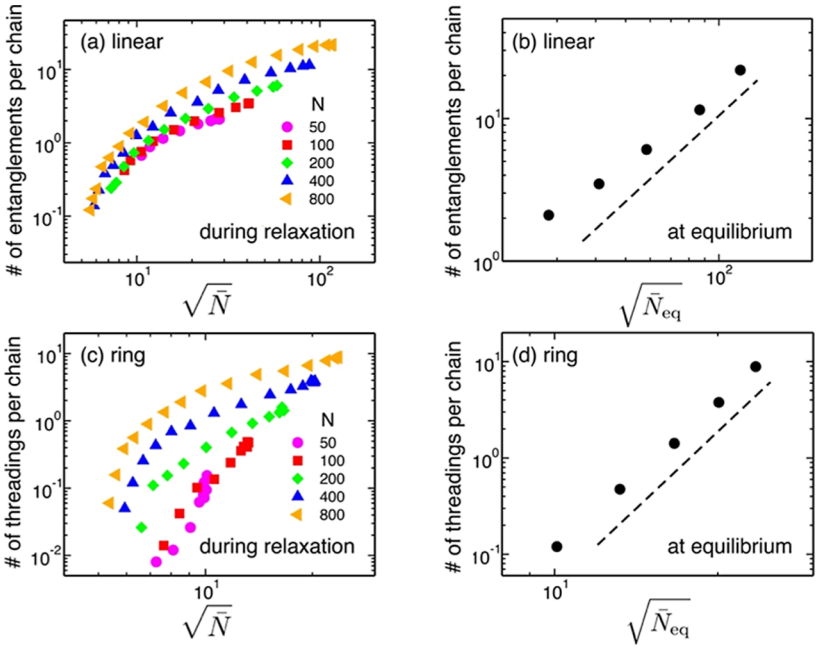

Figure 18. Number of entanglements (a) and threadings (c) per chain as a function of root of the invariant degree of polymerization, $\sqrt{\bar{N}}$, for the initially disentangled linear and ring polymers during their melting, respectively. (b) and (d) Effect of the root of the invariant degree of polymerization of the linear (b) and ring (d) polymers at equilibrated melts, $\sqrt{\bar{N}_{eq}}$, on the number of entanglements and threadings per chain.

formation of an increasing number of entanglements along the chain.

To provide quantitative information concerning the kinetics of topological state formation, Figure 16a,b gives the evolution of the number of entanglements per chain and number of ring−ring threadings averaged per ring as a function of the rescaled time, t/τ_{gc}, during the melting of the initially disentangled linear and ring polymers, respectively. We find that both the number of entanglements and threadings per chain get increases with the progression of the melting, while those systems with larger chain lengths are more strongly entangled or threaded. Correspondence between the kinetics of emergence of the topological states and conformational changes of polymers can be understood by looking into the results given in Figure 16c,d for the systems of N = 800. Analogous to the evolution behavior of g_{inter} $(r = 0)$, a burst of formation of entanglements or threadings in the linear or ring systems, i.e., stage II, takes place concurrently with chain expansion and chain intermixing. Evolution of probability distributions of the number of entanglements and threadings per chain for both cases during their melting is given in Figure 17, from which one can also directly see the emergence of those topological states with time. Very consistent with molecular pictures revealed in Section 3.1, it can be learned from Figure 17 that a burst of topological states, either entanglements or threadings, starts near the end of stage I, the right preparation stage for stage II, when chains expand in the fastest manner. Furthermore, one can notice a saturation of distributions of the number of entanglements or threadings per ring near the end of stage II. All of these findings essentially imply that the emergence of these interesting topological states (e.g., entanglements in the linear systems, and threadings in the rings) essentially stems from a cooperation of chain expansions and interpenetrations.

Considering the decisive role of chain interpenetration in the formation of the topological states,[6,8,12,13,32,57−60] it is now instructive to examine how the number of entanglements and threadings evolve in the course of intertwining of chains during the melting. Figure 18a,c provides the evolution of these topological states as a function of root of the degree of chain interpenetration, $\sqrt{\bar{N}}$, during the melting of initially disentangled linear and ring polymers, respectively. Here, we define the invariant degree of polymerization,[7] $\bar{N}$, as $\bar{N} \equiv (\rho_0 V_c/N)^2$,

https://doi.org/10.1021/acs.macromol.5c01047
Macromolecules 2025, 58, 10164−10180

where $V_c = (\sqrt{6}R_g)^3$ denotes pervaded volume of the polymers, and R_g is the instantaneous radius of gyration of the chain at a given time during the melting process, which can be calculated from the data given in Figure 4a,b. As expected, the number of either entanglements (in the linear case) or threadings (in the rings) increases as chains become more intertwined, i.e., a larger value of $\sqrt{N}$. In detail, it is found that there seems to exist a universal relationship, in a very rough sense, between the number of entanglements formed and the degree of chain interpenetration during the relaxation (i.e., melting) of initially disentangled linear polymers. The existence of a universal relationship between the number of entanglements and the degree of polymer interpenetration in a nonequilibrium process is very interesting, since it is reminiscent of experimental observations that the number of entanglements per chain in an equilibrium melt is also universally determined by the invariant degree of polymerization of the chains.[6,57−60] In the ring case (Figure 18c), however, such a universal behavior does not hold anymore. Figure 18b,d gives the effect of root of the degree of chain interpenetration of the systems at equilibrated melts, $\sqrt{\bar{N}_{eq}}$, on the number of entanglements (or threadings) per chain in equilibrium of linear (or ring) polymers. We note that varying values of $\sqrt{\bar{N}_{eq}}$ correspond to different systems with increasing chain lengths (ranging from 50 to 800). It is concluded that approximately the number of entanglements per chain in the equilibrated linear melts is linearly proportional to $\bar{N}_{eq}$ (denoted by the dashed line). This finding is in good agreement with conclusions previously revealed in experiments.[57−60] For the rings, in contrast, we found that the number of threadings per chain depends on $\sqrt{\bar{N}_{eq}}$ following a different scaling behavior (denoted by the dashed line in Figure 18d), i.e., the number of threadings per chain $\sim(\sqrt{\bar{N}_{eq}})^{5.3}$.

4. CONCLUSIONS

In this work, we carried out extensive molecular dynamics simulations of the melting process of the initially disentangled polymers with varying chain lengths (N being up to 800) in melts, where two kinds of cases, linear and ring, have been considered. The main purpose of this study is to uncover kinetic features and clarify the underlying molecular mechanisms of the melting process, with an emphasis on illuminating specific role of chain topology therein. Meanwhile, we endeavor to clarify, if possible, some interesting issues concerning chain explosions in the course of the melting. Our computational investigation revealed that the melting of initially disentangled polymers, either linear ones or rings, is featured as a three-stage procedure (stage I, stage II, and stage III). During the melting, the polymers experience a synergy of such nonequilibrium processes as conformational changes (globule−coil transitions) of polymer chains, polymer interpenetration, and then formation of nontrivial topological states (i.e., entanglements in the case of linear chains, and chain threadings for ring polymers) of polymers. Furthermore, we found that the melting of initially disentangled linear polymers is accomplished through chain explosion evidenced by our simulation results that (1) total time needed for completion of the melting, τ_{ge}, remains much shorter than the longest relaxation time of the system and (2) radius of gyration of the chains evolves with time following a uniform scaling law at stage II. For the ring case, in contrast, the molecular picture of chain explosion during the melting is obscure. Furthermore, a difference in chain topology results in distinction of molecular details underlying the melting process. Specifically, in the linear case, it is through sufficient "releasing" of the two chain ends that the disentangled linear chains become able to explode for arriving at their well-equilibrated coil conformations, while chain expansion of ring polymers during the melting occurs with the aid of formation of more wrinkled conformations due to the absence of chain ends. Moreover, it is concluded that a concomitant development of polymer interpenetrations essentially acts as a requisite for the occurrence of chain expansion during the melting. Last but not least, the emergence of the interesting topological states (e.g., entanglements in the linear systems, and threadings in the rings) stems from a cooperation of chain expansions and interpenetrations.

AUTHOR INFORMATION

Corresponding Authors

Hong Liu − *Key Laboratory of Theoretical Chemistry of Environment Ministry of Education, School of Environment, South China Normal University, Guangzhou 510006, China*; orcid.org/0000-0002-7256-5751; Email: hongliu@m.scnu.edu.cn;

Jiajia Zhou − *South China Advanced Institute for Soft Matter Science and Technology, School of Emergent Soft Matter, South China University of Technology, Guangzhou 510640, China*; orcid.org/0000-0002-2258-6757; Email: zhouj2@scut.edu.cn;

Xianbo Huang − *National-Certified Enterprise Technology Center, Kingfa Science and Technology Co., LTD., Guangzhou 510006, China*; Email: huangxianbo@kingfa.com.cn;

Guojie Zhang − *School of Chemistry and Chemical Engineering, Guangzhou University, Guangzhou 510006, China*; orcid.org/0009-0005-7822-7525; Email: guojie.zhang@gzhu.edu.cn

Authors

Zhiyuan Cheng − *School of Chemistry and Chemical Engineering, Guangzhou University, Guangzhou 510006, China; Key Laboratory of Theoretical Chemistry of Environment Ministry of Education, School of Environment, South China Normal University, Guangzhou 510006, China*

Li Peng − *National-Certified Enterprise Technology Center, Kingfa Science and Technology Co., LTD., Guangzhou 510006, China*

Bo Yang − *National-Certified Enterprise Technology Center, Kingfa Science and Technology Co., LTD., Guangzhou 510006, China*

Complete contact information is available at: https://pubs.acs.org/10.1021/acs.macromol.5c01047

Notes

The authors declare no competing financial interest.

ACKNOWLEDGMENTS

This work was financially supported by the National Natural Science Foundation of China (Grant No. 21873023).

REFERENCES

(1) de Gennes, P. G. *Scaling Concepts in Polymer Physics*; Cornell University Press: Ithaca, 1979.
(2) Doi, M.; Edwards, S. F. *The Theory of Polymer Dynamics*; Oxford University Press: New York, 1986.
(3) Grosberg, A. Y.; Khokhlov, A. R. *Statistical Physics of Macromolecules*; AIP: New York, 1994.
(4) Rubinstein, M.; Colby, R. H. *Polymer Physics.*; Oxford University Press: New York, 2003
(5) Wang, Z.-G. 50th anniversary perspective: Polymer conformation: A pedagogical review. *Macromolecules* **2017**, *50*, 9073−9114.
(6) Qin, J. Similarity of Polymer Packing in Melts Is Dictated by $\bar{N}$. *Macromolecules* **2024**, *57*, 1885−1892.
(7) $\bar{N}$ was initially defined as $\bar{N} \equiv (\rho R_e^3/N)^2$, Where ρ, R_e, N denote the number density of monomers, end-to-end distance and chain length of the polymers, respectively. For ring polymers considered in this work, however, definition of the end-to-end distance is not applied any more.
(8) Kruteva, M.; Allgaier, J.; Richter, D. Topology Matters: Conformation and Microscopic Dynamics of Ring Polymers. *Macromolecules* **2023**, *56*, 7203−7229.
(9) Halverson, J. D.; Lee, W. B.; Grest, G. S.; Grosberg, A. Y.; Kremer, K. Molecular dynamics simulation study of nonconcatenated ring polymers in a melt. I. Statics. *J. Chem. Phys.* **2011**, *134*, 204904.
(10) Sakaue, T. Ring Polymers in Melts and Solutions: Scaling and Crossover. *Phys. Rev. Lett.* **2011**, *106*, 167802.
(11) Rosa, A.; Everaers, R. Ring Polymers in the Melt State: The Physics of Crumpling. *Phys. Rev. Lett.* **2014**, *112*, 118302.
(12) Tsalikis, D. G.; Mavrantzas, V. G. Threading of Ring Poly(ethylene oxide) Molecules by Linear Chains in the Melt. *ACS Macro Lett.* **2014**, *3*, 763−766.
(13) Smrek, J.; Grosberg, A. Y. Minimal Surfaces on Unconcatenated Polymer Rings in Melt. *ACS Macro Lett.* **2016**, *5*, 750−754.
(14) G Cunha, M. A.; Robbins, M. O. Effect of Flow-Induced Molecular Alignment on Welding and Strength of Polymer Interfaces. *Macromolecules* **2020**, *53*, 8417−8427.
(15) Rastogi, S.; Lippits, D. R.; Peters, G. W. M.; Graf, R.; Yao, Y.; Spiess, H. W. Heterogeneity in polymer melts from melting of polymer crystals. *Nat. Mater.* **2005**, *4*, 635.
(16) Christakopoulos, F.; Troisi, E.; Friederichs, N.; Vermant, J.; Tervoort, T. A. "Tying the Knot": Enhanced Recycling through Ultrafast Entangling across Ultrahigh Molecular Weight Polyethylene Interfaces. *Macromolecules* **2021**, *54*, 9452−9460.
(17) Adhikari, S.; Durning, C. J.; Fish, J.; Simon, J.-W.; Kumar, S. K. Modeling Thermal Welding of Semicrystalline Polymers. *Macromolecules* **2022**, *55*, 1719−1725.
(18) Ge, T.; Pierce, F.; Perahia, D.; Grest, G. S.; Robbins, M. O. Molecular Dynamics Simulations of Polymer Welding: Strength from Interfacial Entanglements. *Phys. Rev. Lett.* **2013**, *110*, 098301.
(19) Wool, R. P.; Yuan, B. L.; McGarel, O. J. Welding of polymer interfaces. *Polym. Eng. Sci.* **1989**, *29*, 1340−1367.
(20) Roy, D.; Roland, C. M. Reentanglement Kinetics in Polyisobutylene. *Macromolecules* **2013**, *46*, 9403−9408.
(21) Dealy, J. M.; Tsang, W. Structural Time Dependency in the Rheological Behavior of Molten Polymers. *J. Appl. Polym. Sci.* **1981**, *26*, 1149−1158.
(22) Stratton, R. A.; Butcher, A. F. Stress Relaxation upon Cessation of Steady Flow and the Overshoot Effect of Polymer Solutions. *J. Polym. Sci. Polym. Phys. Ed.* **1973**, *11*, 1747−1758.
(23) Robertson, C. G.; Warren, S.; Plazek, D. J.; Roland, C. M. Reentanglement Kinetics in Sheared Polybutadiene Solutions. *Macromolecules* **2004**, *37*, 10018−10022.
(24) Krajenta, J.; Safandowska, M.; Pawlak, A. The re-entangling of macromolecules in polypropylene. *Polymer* **2019**, *175*, 215−226.
(25) Teng, C.; Gao, Y.; Wang, X.; Jiang, W.; Zhang, C.; Wang, R.; Zhou, D.; Xue, G. Reentanglement Kinetics of Freeze-Dried Polymers above the Glass Transition Temperature. *Macromolecules* **2012**, *45*, 6648−6651.
(26) Lemstra, P. J.; van Aerle, N. A. M. J.; Bastiaansen, C. W. M. Chain-extended polyethylene. *Polym. J.* **1987**, *19*, 85−98.
(27) Bastiaansen, C. W. M.; Meyer, H. E. H.; Lemstra, P. J. Memory effects in polyethylenes: influence of processing and crystallization history. *Polymer* **1990**, *31*, 1435−1440.
(28) Barham, P. J.; Sadler, D. M. A neutron scattering study of the melting behavior of polyethylene single crystals. *Polymer* **1991**, *32*, 393−395.
(29) de Gennes, P. G. "Explosion" upon melting. *C. R. Acad. Sci. Paris, Ser. 2b* **1995**, *321*, 363−365.
(30) Chen, R.; Jiang, S.; Luo, C. Reconstruction of the entanglement network and its effect on the crystallization and mechanical strength of sintered polymers. *Macromolecules* **2023**, *56*, 5237−5247.
(31) Vettorel, T.; Kremer, K. Development of Entanglements in a Fully Disentangled Polymer Melt. *Macromol. Theory Simul.* **2010**, *19*, 44−56.
(32) Michieletto, D.; Turner, M. S. A topologically driven glass in ring polymers. *Proc. Natl. Acad. Sci. U.S.A.* **2016**, *113*, 5195−5200.
(33) Halverson, J. D.; Smrek, J.; Kremer, K.; Grosberg, A. Y. From a melt of rings to chromosome territories: the role of topological constraints in genome folding. *Rep. Prog. Phys.* **2014**, *77*, 022601.
(34) Kremer, K.; Grest, G. S. Dynamics of entangled linear polymer melts: a molecular-dynamics simulation. *J. Chem. Phys.* **1990**, *92*, 5057.
(35) Zhang, G. J.; Moreira, L. A.; Stuehn, T.; Daoulas, K. Ch.; Kremer, K. Equilibration of high molecular weight polymer melts: a hierarchical strategy. *ACS Macro Lett.* **2014**, *3*, 198−203.
(36) Zhang, G. J.; Stuehn, T.; Daoulas, K. Ch.; Kremer, K. Communication: one size fits all: Equilibrating chemically different polymer liquids through universal long-wavelength description. *J. Chem. Phys.* **2015**, *142*, 221102.
(37) Moreira, L. A.; Zhang, G. J.; Muller, F.; Stuehn, T.; Kremer, K. Direct equilibration and characterization of polymer melts for computer simulations. *Macromol. Theory Simul.* **2015**, *24*, 419−431.
(38) Zhang, G. J.; Chazirakis, A.; Harmandaris, V. A.; Stuehn, T.; Daoulas, K. Ch.; Kremer, K. Hierarchical modelling of polystyrene melts: from soft blobs to atomistic resolution. *Soft Matter* **2019**, *15*, 289.
(39) Halverson, J. D.; Lee, W. B.; Grest, G. S.; Grosberg, A. Y.; Kremer, K. Molecular dynamics simulation study of non-concatenated ring polymers in a melt. II. Dynamics. *J. Chem. Phys.* **2011**, *134*, 204905.
(40) Cai, X.; Liang, C.; Liu, H.; Zhang, G. J. Conformation and structure of ring polymers in semidilute solutions: A molecular dynamics simulation study. *Polymer* **2022**, *253*, 124953.
(41) Rauscher, P. M.; Rowan, S. J.; de Pablo, J. J. Topological effects in isolated poly[n]catenanes: molecular dynamics simulations and Rouse mode analysis. *ACS Macro Lett.* **2018**, *7*, 938−943.
(42) Wu, Z.-T.; Zhou, J.-J. Mechanical Properties of Interlocked-ring Polymers: A Molecular Dynamics Simulation Study. *Chin. J. Polym. Sci.* **2019**, *37*, 1298−1304.
(43) Rauscher, P. M.; Schweizer, K. S.; Rowan, S. J.; de Pablo, J. J. Thermodynamics and structure of poly[n]catenane melts. *Macromolecules* **2020**, *53*, 3390−3408.
(44) Rauscher, P. M.; Schweizer, K. S.; Rowan, S. J.; de Pablo, J. J. Dynamics of poly[n]catenane melts. *J. Chem. Phys.* **2020**, *152*, 214901.
(45) Zhang, G. J.; Zhang, J. G. Topological catenation induced swelling of ring polymers revealed by molecular dynamics simulation. *Polymer* **2020**, *196*, 122475.
(46) Lei, H. Q.; Zhang, J. G.; Wang, L. M.; Zhang, G. J. Dimensional and shape properties of a single linear polycatenane: Effect of catenation topology. *Polymer* **2021**, *212*, 123160.
(47) Li, J.; Gu, F.; Yao, N.; Wang, H.; Liao, Q. Double Asymptotic Structures of Topologically Interlocked Molecules. *ACS Macro Lett.* **2021**, *10*, 1094−1098.
(48) Chiarantoni, P.; Micheletti, C. Effect of Ring Rigidity on the Statics and Dynamics of Linear Catenanes. *Macromolecules* **2022**, *55*, 4523−4532.

https://doi.org/10.1021/acs.macromol.5c01047
Macromolecules 2025, 58, 10164−10180

(49) Chen, Y. X.; Cai, X. Q.; Zhang, G. J. Topological Catenation Enhances Elastic Modulus of Single Linear Polycatenane. *Chin. J. Polym. Sci.* **2023**, *41*, 1486−1496.
(50) Chen, Y.; Xu, D.; Rao, Y.; Zhang, G. J. Nonlinear Elasticity of Single Linear Polycatenane: Emergence of Stress-Softening. *Macromolecules* **2024**, *57*, 9041−9058.
(51) Everaers, R.; Sukumaran, S. K.; Grest, G. S.; Svaneborg, C.; Sivasubramanian, A.; Kremer, K. Rheology and Microscopic Topology of Entangled Polymeric Liquids. *Science* **2004**, *303*, 823.
(52) Sukumaran, S. K.; Grest, G. S.; Kremer, K.; Everaers, R. Identifying the Primitive Path Mesh in Entangled Polymer Liquids. *J. Polym. Sci., Part B: Polym. Phys.* **2005**, *43*, 917−933.
(53) Note That the Scaling Behavior, $\alpha \approx 3.4$, May or May Not Hold When $N > 800$. A Careful Investigation of the Scaling Laws, if Existing, of $\tau_{gc}$with Respect to Chain Length for Systems with $N > 800$ is However Out of the Scope of the Present Computational Work.
(54) Tang, J.; Du, N.; Doyle, P. S. Compression and self-entanglement of single DNA molecules under uniform electric field. *Proc. Natl. Acad. Sci. U.S.A.* **2011**, *108*, 16153−16158.
(55) Tsolou, G.; Stratikis, N.; Baig, C.; Stephanou, P. S.; Mavrantzas, V. G. Melt Structure and Dynamics of Unentangled Polyethylene Rings: Rouse Theory, Atomistic Molecular Dynamics Simulation, and Comparison with the Linear Analogues. *Macromolecules* **2010**, *43*, 10692−10713.
(56) Auhl, R.; Everaers, R.; Grest, G. S.; Kremer, K.; Plimpton, S. J. Equilibration of long chain polymer melts in computer simulations. *J. Chem. Phys.* **2003**, *119*, 12718.
(57) Lin, Y.-H. Number of Entanglement Strands per Cubed Tube Diameter, a Fundamental Aspect of Topological Universality in Polymer Viscoelasticity. *Macromolecules* **1987**, *20*, 3080−3083.
(58) Kavassalis, T. A.; Noolandi, J. New View of Entanglements in Dense Polymer Systems. *Phys. Rev. Lett.* **1987**, *59*, 2674.
(59) Fetters, L. J.; Lohse, D. J.; Richter, D.; Witten, T. A.; Zirkel, A. Connection between Polymer Molecular Weight, Density, Chain Dimensions, and Melt Viscoelastic Properties. *Macromolecules* **1994**, *27*, 4639.
(60) Fetters, L. J.; Lohse, D. J.; Milner, S. T.; Graessley, W. W. Packing Length Influence in Linear Polymer Melts on the Entanglement, Critical, and Reptation Molecular Weights. *Macromolecules* **1999**, *32*, 6847−6851.

https://doi.org/10.1021/acs.macromol.5c01047
Macromolecules 2025, 58, 10164−10180